IJASST International Journal of Applied Sciences and Smart Technologies

Volume 06
Issue 02

p-ISSN 2655-8564, e-ISSN 2685-943, pp. 241-266, 2024

Density Functional Theory Investigation on The Electronic Structure, Properties and IR Spectra of 9,10-Iphenylanthracene

Owolabi J Adeyemi[1*], Hassan Gambo[1], Onimisi M Yusuf[1], Gidado S Abdulkadir[2], Ali Haruna[1], Bankole J Akinade[3], Akusu C Onma[4], Muhammed L Madugu[1], Sakinat L Usman[1]

[1]*Department of Physics Nigerian Defence Academy, Kaduna, Nigeria*
[2]*Department of Physics Bayero University Kano, Nigeria*
[3]*Department of Physics Federal University lafia, Nigeria*
[4]*Department of Physics Gombe state University Gombe, Nigeria*
[*]*Corresponding Author: jaowolabi@nda.edu.ng*

(Received 18-05-2024; Revised 09-07-2024; Accepted 22-07-2024)

Abstract

9,10-Diphenylanthracene belong to a class of polymer-based materials featuring a π-bonded molecules (organic semiconductors). We conducted a theoretical investigation into 9,10-DPA in both neutral and ionic states using Density Functional Theory (DFT) implemented in the Gaussian 09 package. The calculations employed B3LYP/6-31+G(d) and B3LYP/6-311++G(d,p) basis sets. The study focused on evaluating structural properties, electronic properties, global chemical reactivity descriptors and IR spectra of 9,10-DPA. These assessments aimed to elucidate the reactivity, stability, and conductivity of this molecule. The results reveal that charging influences the structural, electronic, and global index of the molecule. The analysis of bond lengths and angles emphasized that the following bond length R(C7-H18), R(C8-H19), R(C12-H26) and R(C13-H27) exhibits greater bond energy and strength in both neutral and ionic stats because of having shorter bond length than the remaining regardless of the chosen basis set. In the case of energy gap, the anionic alpha molecular orbital exhibits lower stability of having the lowest energy gap of 1.3679eV, indicating higher reactivity and conductivity among the entire MO and is supported by a higher softness value (1.15eV) and higher chemical potential (1.39eV). The cationic beta molecule exhibited stronger electron-attracting power because of having higher electronegativity (9.00eV), lower chemical potential (-9.00eV) and higher electrophilicity index (36.81eV). The vibrational analysis shows that the anionic molecular state possessed the highest IR absorption which occurred at the frequency of 1346.96cm-1. Overall, the findings underscore the importance of charge state in enhancing the electronic properties and the reactivity of these molecules for various applications in the field of organic electronics.

This work is licensed under a Creative Commons Attribution 4.0 International License

Keywords: 9,10-Diphenylanthracene, ionization potential, electron affinity, global chemical index, infrared spectra, density of state

1 Introduction

There has been a lot of interest in entirely organic technologies during the past few decades. Organic transistors and discrete OLED displays have the potential to produce devices with enhanced properties over liquid crystal display technology, including lower power consumption, better resolution, more mechanical flexibility, and lower production costs. To create novel materials with enhanced device performance, it is necessary to comprehend the connection between molecular structural and electrical properties [1].

Organic semiconductor materials have found vast application in light-emitting diodes; photovoltaic cells. This development is because of the strong optical absorption, mechanical flexibility, low cost and solubility these materials exhibit [2].

To be more precise, organic semiconductor devices are less expensive than traditional inorganic semiconductor electronic technologies since they are simpler to manufacture and does not need sophisticated photolithographic processes or high vacuum deposition procedures [3].

Organic semiconductors (OSCs) are solids made of π -bonded molecules or polymers that frequently include carbon and hydrogen atoms as well as heteroatoms like nitrogen, sulphur, and oxygen. They can be found as molecular crystals or amorphous thin films. By nature, they are electrical insulators, but when charges are added using appropriate electrodes during doping or photoexcitation, they become semiconductors [4]. The benefits of organic semiconductors for the production of electronic devices include their low cost, suitability for roll-to-roll processing, ease of fabrication at low temperatures, printable nature, flexible and large area applications due to their mechanical flexibility, and active matrix display backplanes. Additionally, these benefits served as the motivation for using these organic semiconductors [5]. Organic semiconductors, which combined the desirable qualities of metals and polymers with solubility, mechanical strength, and adjustable physicochemical properties, enabled the development of novel devices. However, a lot more cutting-edge studies and

advancements in manufacturing technology are still needed to realize all conductive macromolecules' potential applications [6].

Anthracenes and their derivatives hold a significant place in fundamental physics research among organic materials because the molecules are relatively small and straightforward, making it easier to understand the connections between molecular structures, optical properties, and transport properties in organic semiconductor materials [1].

The chemical activity of a molecule is shown by the highest occupied molecular orbital (HOMO) or singly occupied molecular orbital (SOMO) for the case of radicals, lowest unoccupied molecular orbital (LUMO), and their related energy gaps. A molecule's kinetic stability, chemical reactivity, optical polarizability, and chemical hardness-softness are all governed by the energy difference between LUMO and HOMO/SOMO [2]. Furthermore, in study on the Synthesis and Divergent Electronic Properties of Two Ring-Fused Derivatives of 9,10-Diphenylanthracene, the isomers revealed dissimilar photophysical and redox properties with 2 having a much smaller HOMO−LUMO gap than 1 [7]. The schematic of Molecular structure can be seen in Fig. 1. When considering the movement of electrons or holes in an organic molecular solid, one must keep in mind that ionic molecular states are involved. For instance, an electron must be removed to convert a neutral molecule into a radical cation. This defective electron can move from one molecule to the next [8].

Theoretical investigation of hole mobility in 9,10-diphenylanthracene by density functional calculations also revealed that using the coupling matrix calculated by the CTI method, they predicted a hole mobility of 2.15cm2/(Vs) for Diphenylanthracene (DPA), whereas the CTI method gave the values as 0.35 and 1.39cm2/(Vs) for naphthalene and anthracene, respectively [9].

Additionally, the energy differences between the lowest unoccupied molecular orbital (LUMO) and the highest occupied molecular orbital (HOMO) can be used to estimate the active mobility of polycyclic aromatic hydrocarbons (PAH). The organic molecule can easily give or accept an electron due to its tiny energy gap [10].

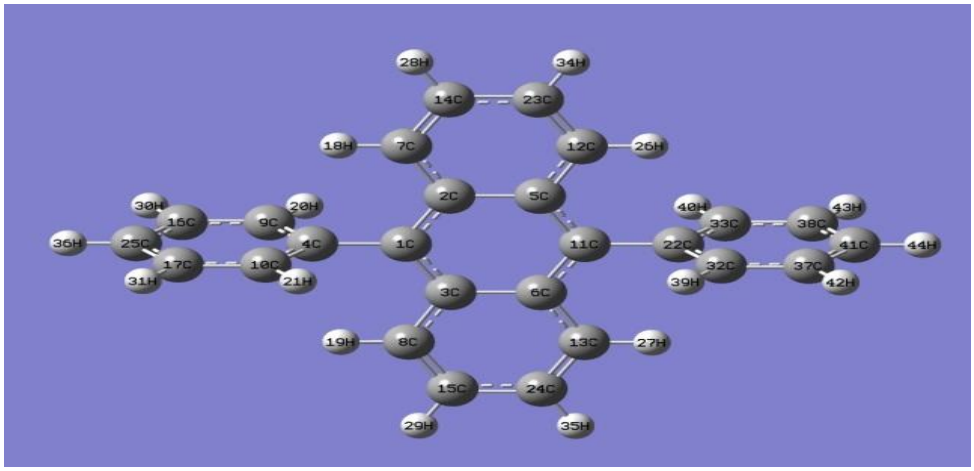

Figure 1. Molecular structure of 9,10-DPA and its derivative 2-bromo-9,10-DPA

In this study, to address some of the gaps in the literature, the electronic structure, properties and IR spectra of the isolated 9,10-DPA in neutral and at different charge states were computed using density functional theory embedded in Gaussian 09 software at two different basis sets b3lyp6-31+G(d) and b3lyp6- 311++ G(d,p).

2 Theoretical Background

Density Functional Theory (DFT)

Density functional theory (DFT) was first put on theoretical footing by Kohn and Hohenberg in the frame work of the two Hohenberg-Kohn theorems in 1964. While in 1965, Kohn and Sham (KS) reformulated in more familiar form and to the practical application of (DFT). [11].

Density functional theory (DFT) is a quantum mechanical method used in physics and chemistry to investigate and calculate the physical properties of atoms, molecules and solids. It is now consider as one of the most important tools for calculating the ground state properties of semiconductors, and to investigate the electronic structure of many electron systems [12]. The quantum mechanical wave function contains all the information about a given system, including the case of a simple 2-D square potential or even a hydrogen atom. One can solve the Schrödinger equation exactly in order to get the wave function of the system and the allowed energy states of the system can be determined. Unfortunately, it is difficult to solve the Schrödinger equation for N-body

system. Evidently, some approximations are involved to render the problem solvable. Kohn et al., (1996) defined Density Functional Theory (DFT) as a theory of electronic structure based on the electron density distribution n(r), instead of many-electron wave function [13]:

However, the electron density n(r) for many-electron system is defined as:

$$n(r) = N \int \left| \psi(r1,r2,r3,\ldots.rN) \right| 2dr2\ldots drN \quad (2.1)$$

where N is the number of electrons, ψ is the many-electron wave function, and r represent the spatial coordinates of the electrons.

The total electron density is then expressed as the squared magnitudes of the Kohn-Sham orbitals.

$$\rho(r) = \sum iN=1 \left| \psi i\ (r) \right| 2 \quad (2.2)$$

where:

ψi (r) = the Kohn-Sham orbitals

ρ(r) = electron density

N = number of electrons in the system

Within DFT, the ground state energy can be determined using the density relation given above [14].

Ionization Potential (IP) And Electron Affinity (EA)

Beyond charge mobility, another crucial factor influencing the performance of organic materials in the context of organic devices is charge injection efficiency. It is an important aspect of organic materials used in various electronic and optoelectronic devices. It ensures that charges (electrons or holes) can effectively transition from the electrode into the organic material. Several parameters including electron affinity and ionization potential, significantly define the charge injection efficiency of organic semiconductors. These parameters play a vital role in facilitating the efficient injection of either electrons or holes into the vacant HOMO-LUMO levels [15].

The ionization potential (IP) represents the energy required to remove an electron from the highest occupied molecular orbital (HOMO) or singly occupied molecular orbital (SOMO) (for radicals), while electron affinity (EA) denotes the energy alteration that occurs when introducing an electron into the lowest unoccupied molecular orbital (LUMO). These properties are closely related to charge injection efficiency, as they define the ease with which charges can be injected into the HOMO-LUMO levels [15].

In the context of molecular orbital theory, there exists a direct relationship between the HOMO/SOMO energy and the ionization potential, as well as the LUMO energy and the electron affinity. This connection is formalized by Koopmans' theorem, which is utilized to estimate these fundamental properties (IP = −EHOMO and EA = –ELUMO).

Koopmans' theorem establishes a direct relationship between HOMO energy and ionization potential (IP) and between LUMO energy and electron affinity (EA). This theorem provides a convenient way to estimate these important electronic properties from quantum mechanical calculations [15].

A molecule's capacity to either accept or release an electron hinges on its ionization potential (IP) and electron affinity (EA). When the electron affinity is low, it becomes more challenging to incorporate an additional electron into the molecule. Conversely, when the ionization potential (IP) is high, the process of removing an electron becomes more difficult [2].

Koopmans' equations can be used to calculate the ionization potential (IP) and electron affinities (EA) of the studied molecule [2]

$$IP = -EHOMO \tag{2.3}$$

$$EA = -ELUMO \tag{2.4}$$

where;

$EHOMO$ = energy of the HOMO

$ELUMO$ = energy of the LUMO

The HOMO-LUMO energy gap (Eg) can be obtained from the relation;

$$Eg = ELUMO - EHOMO \approx IP - EA \tag{2.5}$$

Global Chemical Reactivity Descriptors (GCRD)

Chemical potential, chemical hardness, softness, electronegativity, and electrophilicity index are parameters that aid in predicting and understanding trends in global chemical reactivity. Koopmans' equations can be used to calculate the ionization potential (IP) and electron affinities (EA) of the studied molecule [2];

$$IP = -EHOMO \quad (2.6)$$

$$EA = -ELUMO \quad (2.7)$$

where;

$EHOMO$ = energy of the HOMO

$ELUMO$ = energy of the LUMO

The HOMO-LUMO energy gap (Eg) can be obtained from the relation;

$$Eg = ELUMO - EHOMO \approx IP - EA \quad (2.8)$$

The global chemical reactivity descriptors (GCRDs) can be obtained as follows;

The chemical hardness (η) could be expressed in terms of IP and EA as;

$$\eta = (ELUMO - EHOMO)/2 \approx (IP - EA)/2 \quad (2.9)$$

Chemical softness is given by;

$$s = \frac{1}{\eta} \quad (2.10)$$

The chemical potential is given by;

$$\mu = -\left(\frac{IP+EA}{2}\right) \quad (2.11)$$

The electronegativity is given by;

$$X = \frac{IP+EA}{2} \tag{2.12}$$

Electrophilicity index (ω) - The electrophilicity index measures the amount of energy that is lost as a result of the maximum amount of electron flow between the donor and acceptor. It is expressed as [2];

$$\omega = \frac{\mu^2}{2\eta} \tag{2.13}$$

Computational Method

In this research, the Gaussian 09W package was used to study the electronic structure, properties and IR spectra of 9,10-DPA at different charge states. Optimization of the geometric structure of our target molecule was considered first, thereby allowing every parameter of the ground states to have total freedom to relax and each computation converged to an optimized geometry that corresponds to a true energy minimum. With the optimized geometry, single-point energy calculations of the molecules were performed to obtain parameters such as HOMO (highest occupied molecular orbital), SOMO (singly occupied molecular orbital), LUMO (lowest unoccupied molecular orbital) and total ground state energy were calculated using density functional theory (DFT) method with the three-parameter hybrid exchange functional of Becke and Lee-Yang-Parr correlation functional (B3LYP) [16] using the two basis sets {6-31+G (d) and 6-311++G (d, p)}. Other parameters like HOMO-LUMO energy gap, ionization potential, electron affinity as well as global chemical reactivity descriptors (such as chemical hardness, softness, electronegativity, chemical potential and electrophilicity index) and the vibrational frequencies of the target molecules were also calculated, while the IR spectra was computed from the vibrational frequencies using Gauss view package. The same procedure was also adopted for the computation of the ionic (anionic and cationic) molecules by changing the charge state from 0 to -1 and +1 respectively. All calculations

were carried out under the Gaussian 09 software program coding for Density Functional Theory (DFT).

3 Results and Discussions

Optimized Bond Length of 9,10- Diphenylanthracene

Tables 1 present data regarding bond lengths for 9,10-DPA, calculated based on DFT method using B3LYP level of theory with the 6-31+G(d) and 6-311++G(d,p) basis sets. Bond length represents the distance between two atoms covalently bonded in a molecule. The energy associated with molecules featuring shorter bond lengths is stronger compared to those with longer bond lengths [2].

The results shows that the calculated bond lengths of 9,10-DPA were found to be the least with the following values; (1.0849Å), (1.0834Å) and (1.0865Å) when using B3LYP/6-3+1G and (1.0823Å), (1.081Å) and (1.0837Å) while using B3LYP/6-311++G for neutral, cationic and anionic respectively at the following; R(C_7-H_{18}), R(C_8-H_{19}), R(C_{12}-H_{26}) and R(C_{13}-H_{27}). The bond lengths in R(C_1-C_4) and R(C_{11}-C_{22}) were found to be the highest with the following values; (1.4988Å), (1.484Å) and (1.4958Å) upon using B3LYP/6-3+1G and (1.4937Å), (1.483Å) and (1.4947Å) when B3LYP/6-311++G was used respectively. From these results, we can observed that the strongest bond was found in the cationic state which occurred at B3LYP/6-311++G level of theory for R(C_7-H_{18}), R(C_8-H_{19}), R(C_{12}-H_{26}) and R(C_{13}-H_{27}) with the value (1.081Å), while the weakest bond was found in the neutral state, occurred at B3LYP/6-31+G level of theory for R(C_1-C_4) and R(C_{11}-C_{22}) with the value of (1.4988Å). Both values were in agreement with the experimental values of (1.085Å) and (1.437Å) respectively for anthracene [17].

Table 1. Bond Length (Å) of 9,10-Diphenylanthracene

BOND LENGTHS (Å) OF 9,10-DIPHENYLANTHRACENE						
	B3LYP/6-31+G(d)			**B3LYP/6-311++G(d,p)**		
	Neutral	**Cationic**	**Anionic**	**Neutral**	**Cationic**	**Anionic**
R(C1-C2)	1.4125	1.4296	1.4259	1.4092	1.4264	1.4226
R(C1-C3)	1.4124	1.4296	1.426	1.4091	1.4264	1.4226
R(C1-C4)	1.4988	1.484	1.4958	1.4937	1.483	1.4947
R(C2-C5)	1.4479	1.4425	1.4526	1.4455	1.4398	1.4505
R(C2-C7)	1.4344	1.4191	1.4234	1.4321	1.4163	1.4209
R(C3-C6)	1.4479	1.4425	1.4526	1.4455	1.4398	1.4505
R(C3-C8)	1.4344	1.4191	1.4235	1.4321	1.4162	1.4209

R(C4-C9)	1.4037	1.4084	1.4063	1.4001	1.4045	1.4026
R(C4-C10)	1.4037	1.4084	1.4063	1.4001	1.4045	1.4027
R(C5-C11)	1.4125	1.4296	1.426	1.4092	1.4263	1.4226
R(C5-C12)	1.4344	1.4191	1.4234	1.4321	1.4162	1.4209
R(C6-C11)	1.4125	1.4296	1.4259	1.4092	1.4263	1.4226
R(C6-C13)	1.4344	1.4191	1.4235	1.4321	1.4162	1.4209
R(C7-C14)	1.3714	1.3886	1.3953	1.367	1.3848	1.3918
R(C7-H18)	1.0849	1.0834	1.0865	1.0823	1.081	1.0837
R(C8-C15)	1.3713	1.3886	1.3953	1.367	1.3848	1.3918
R(C8-H19)	1.0849	1.0834	1.0865	1.0823	1.081	1.0837
R(C9-H16)	1.3977	1.3951	1.3984	1.3941	1.3915	1.3948
R(C9-H20)	1.0875	1.0868	1.0877	1.0846	1.0841	1.0848
R(C10-C17)	1.3977	1.3951	1.3984	1.3941	1.3916	1.3947
R(C10-H21)	1.0875	1.0868	1.0877	1.0846	1.0841	1.0848
R(C11-C22)	1.4988	1.484	1.4958	1.4976	1.4831	1.4947
R(C12-C23)	1.3713	1.3886	1.3953	1.367	1.3848	1.3918
R(C12-H26)	1.0849	1.0834	1.0865	1.0823	1.081	1.0837
R(C13-C24)	1.3713	1.3886	1.3953	1.367	1.3848	1.3918
R(C13-H27)	1.0849	1.0834	1.0865	1.0823	1.081	1.0837
R(C14-C23)	1.4236	1.4041	1.4029	1.421	1.401	1.3994
R(C14-H28)	1.0871	1.0859	1.0892	1.0843	1.0834	1.0862
R(C15-C24)	1.4236	1.4041	1.403	1.421	1.401	1.3994
R(C15-H29)	1.0871	1.0859	1.0892	1.0843	1.0834	1.0862
R(C16-C25)	1.3978	1.3984	1.3986	1.3939	1.3946	1.3947
R(C16-H30)	1.0873	1.0863	1.0888	1.0845	1.0836	1.0859
R(C17-C25)	1.3978	1.3984	1.3986	1.3939	1.3946	1.3948
R(C17-H31)	1.0873	1.0863	1.0888	1.0845	1.0836	1.0859
R(C22-C32)	1.4037	1.4084	1.4063	1.4001	1.4045	1.4026
R(C22-C33)	1.4037	1.4084	1.4063	1.4001	1.4045	1.4026
R(C23-H34)	1.0871	1.0859	1.0892	1.0843	1.0834	1.0862
R(C24-H35)	1.0871	1.0859	1.0892	1.0843	1.0834	1.0862
R(C25-H36)	1.0871	1.0862	1.0885	1.0842	1.0835	1.0855
R(C32-C37)	1.3977	1.3951	1.3984	1.3941	1.3916	1.3948
R(C32-H39)	1.0875	1.0868	1.0877	1.0846	1.0841	1.0848
R(C33-C38)	1.3977	1.3951	1.3984	1.3941	1.3916	1.3948
R(C33-H40)	1.0875	1.0868	1.0877	1.0846	1.0841	1.0848
R(C37-C41)	1.3978	1.3985	1.3986	1.3939	1.3945	1.3948
R(C37-H42)	1.0873	1.0863	1.0888	1.0845	1.0836	1.0859
R(C38-C41)	1.3978	1.3984	1.3986	1.3939	1.3945	1.3948
R(C38-H43)	1.0873	1.0863	1.0888	1.0845	1.0836	1.0859
R(C41-H44)	1.0871	1.0862	1.0885	1.0842	1.0835	1.0855

Optimized Bond Angles of 9,10- Diphenylanthracene

Other structural properties that define molecular geometries of an organic material are; bond angles and torsional angles. A bond angle is the angle formed between three atoms across at least two bonds [15]. The optimized bond angles of 9,10-DPA at the DFT levels of theory within the basis sets were summarized and presented in Table 2. The calculated bond angles for 9,10-DPA at B3LYP/6-31+G and B3LPY/6-311++G were

found to be in good agreement with the experimental values, and it showed small deviations at some points of the basis sets.

Table 2. Bond Angle (0) of 9,10-Diphenylanthracene

BOND ANGLE (^{0}) OF 9,10-DIPHENYLANTHRACENE						
	B3LYP/6-31+G(d)			B3LYP/6-31+1+G(d,p)		
	Neutral	Cationic	Anionic	Neutral	Cationic	Anionic
A(C2,C1,C3)	120.0465	119.3374	121.4131	120.0458	119.3671	121.4307
A(C2,C1,C4)	119.9787	120.3318	119.2918	119.9787	120.3135	119.2833
A(C3,C1,C4)	119.9749	120.3308	119.2951	119.9755	120.3194	119.286
A(C1,C2,C5)	119.9762	120.2885	119.2949	119.9766	120.2768	119.2858
A(C1,C2,C7)	121.7693	121.2662	122.672	121.7852	121.2637	122.6917
A(C5,C2,C7)	118.2584	118.4415	118.0333	118.2382	118.4554	118.0225
A(C1,C3,C6)	119.9773	120.2887	119.2925	119.9775	120.2742	119.2838
A(C1,C3,C8)	121.767	121.2658	122.6744	121.7832	121.2669	122.6937
A(C6,C3,C8)	118.2558	118.4417	118.0331	118.2393	118.4549	118.0225
A(C1,C4,C9)	120.7137	120.5091	121.2475	120.6927	120.4656	121.2179
A(C1,C4,C10)	120.7124	120.5082	121.244	120.6915	120.4674	121.2143
A(C9,C4,C10)	118.5739	118.9827	117.5085	118.6158	119.067	117.5677
A(C2,C5,C11)	119.9771	120.2885	119.2921	119.9774	120.2752	119.2833
A(C2,C5,C12)	118.2557	118.4413	118.0337	118.2393	118.4587	118.0232
A(C11,C5,C12)	121.7671	121.2664	122.6742	121.7834	121.2622	122.6935
A(C3,C6,C11)	119.9756	120.2884	119.2946	119.9769	120.2775	119.2857
A(C3,C6,C13)	118.2545	118.4411	118.0337	118.2382	118.4586	118.023
A(C11,C6,C13)	121.769	121.2666	122.6717	121.7849	121.26	122.6913
A(C2,C7,C14)	121.4787	121.3704	122.1477	121.4536	121.3089	122.1098
A(C2,C7,H18)	118.6362	119.2644	118.6772	118.6213	119.2239	118.6885
A(C14,C7,H18)	119.8851	119.3646	119.1751	119.9251	119.4669	119.2017
A(C3,C8,C15)	121.4783	121.3704	122.1481	121.4533	121.3099	122.1103
A(C3,C8,H19)	118.6357	119.2644	118.6774	118.6209	119.2249	118.6884
A(C15,C8,H19)	119.886	119.3647	119.1745	119.9258	119.4649	119.2013
A(C4,C9,C16)	120.7615	120.3788	121.4301	120.7234	120.3189	121.3811
A(C4,C9,H20)	119.2845	119.7398	118.5646	119.3163	119.8046	118.5797
A(C16,C9,H20)	119.954	119.8572	120.0053	119.9602	119.854	120.0382
A(C4,C10,C17)	120.7611	120.3788	121.4296	120.7231	120.3188	121.3805
A(C4,C10,H21)	119.2834	119.7398	118.5619	119.3151	119.8048	118.5769
A(C17,C10,H21)	119.9555	119.8573	120.0085	119.9618	119.8537	120.0426
A(C5,C11,C6)	120.0464	119.3377	121.413	120.0458	119.3696	121.4306
A(C5,C11,C22)	119.975	120.3308	119.2938	119.9756	120.3165	119.2847
A(C6,C11,C22)	119.9785	120.3314	119.2931	119.9786	120.3139	119.2847
A(C5,C12,C23)	121.4783	121.3704	122.1477	121.4532	121.3092	122.1099
A(C5,C12,H26)	118.636	119.2643	118.6783	118.6212	119.2233	118.6894
A(C23,C12,H26)	119.8857	119.3647	119.174	119.9256	119.4671	119.2007
A(C6,C13,C24)	121.4783	121.3704	122.1473	121.4533	121.3088	122.1094
A(C6,C13,H27)	118.6364	119.2643	118.6771	118.6215	119.2225	118.6883
A(C24,C13,H27)	119.8853	119.3647	119.1755	119.9252	119.4684	119.2023
A(C7,C14,C23)	120.2663	120.0873	119.8192	120.3077	120.1373	119.8676
A(C7,C14,H28)	119.9763	119.7506	119.7327	119.99	119.7731	119.7608
A(C23,C14,H28)	119.7574	120.1609	120.4482	119.7022	120.0885	120.3715
A(C8,C15,C24)	120.2663	120.0872	119.8183	120.3077	120.138	119.8667

A(C8,C15,H29)	119.9764	119.7506	119.7344	119.9901	119.7729	119.7627
A(C24,C15,H29)	119.7573	120.161	120.4473	119.7021	120.0881	120.3706
A(C9,C16,C25)	120.1591	120.1761	120.1762	120.1698	120.1831	120.1888
A(C9,C16,H30)	119.7052	119.6445	119.788	119.7364	119.6671	119.8132
A(C25,C16,H30)	120.1357	120.1793	120.0359	120.0938	120.1499	119.998
A(C10,C17,C25)	120.1594	120.1761	120.1766	120.1701	120.1833	120.1893
A(C10,C17,H31)	119.7055	119.6444	119.7911	119.7368	119.6665	119.8165
A(C25,C17,H31)	120.1351	120.1794	120.0323	120.0931	120.1503	119.9942
A(C11,C22,C32)	120.7132	120.5079	121.246	120.6923	120.4656	121.2164
A(C11,C22,C33)	120.7128	120.509	121.2457	120.6919	120.4645	121.2161
A(C32,C22,C33)	118.574	118.983	117.5082	118.6159	119.0698	117.5675
A(C12,C23,C14)	120.2665	120.0874	119.8185	120.3079	120.1371	119.8669

The bond angle in 9,10-DPA formed at B3LYP/6-31G level of theory for A(3,6,13) in neutral and cationic state and A(32,22,33) in anionic state with the values (118.2545^0), (118.4411^0) and (117.5082^0) respectively as well as B3LYP/6-311++G level of theory for A(5,2,7) and A(3,6,13) in neutral, A(6,3,8) in cationic and A(32,22,33) in anionic state with the following values (118.2382^0), (118.4547^0) and (117.5675^0) were the smallest and ware in agreement with the other experimental values (112^0-118.8^0) for anthracene [17]. It was observed that some bond angles in table 2 were found to be more than 118.8^0, these slight increments were attributed to ionizing and large steric hindrance as a result of substitution of one hydrogen atom with the functional molecule (phenyl group) at the central rings of anthracene structure [18].

Molecular Orbitals

The HOMO (Highest Occupied Molecular Orbital) energy is indicative of a molecule's ability to donate electrons, whereas the LUMO (Lowest Unoccupied Molecular Orbital) energy reflects its capacity to accept electrons. In molecular orbital theory, the HOMO and LUMO play crucial roles in understanding the reactivity of a molecule. The energy gap between the LUMO and HOMO, often referred to as the HOMO-LUMO energy gap, is a key determinant of a molecule's reactivity and conductivity, as a smaller gap suggests greater reactivity due to easier electron transfer [15].

The band gap is an essential property for characterizing the electrical structures of solids. Regard to this, a study has systematically examined how the band gap changes for anthracene at pressures ranging from 0 to 27GPa. They discovered that the band gap for

solid anthracene at ambient pressure is 2.2eV at the generalized gradient approximation (GGA) level, which is a little higher than the Local Density Approximations (LDA) value of 1.9eV [19].

Table 3 in our study provides insight into HOMO (Highest Occupied Molecular Orbital), SOMO (Singly Occupied Molecular Orbital), LUMO (Lowest Unoccupied Molecular Orbital) and HOMO/SOMO-LUMO gap (energy gap) values for both neutral and ionic forms of 9,10-DPA. These calculations were conducted using the two different basis sets (6-31+G(d) and 6-311++G(d,p). It is well-established that compounds with smaller HOMO-LUMO energy gap values tend to exhibit higher reactivity and greater conductivity because it requires a small amount of energy for electron to transition from HOMO to the LUMO or to transition from the ground state to the excited state indicating its easiness in the charge injection making it a better choice for organic materials used in organic semiconductor applications such as organic light emitting diodes, organic photovoltaic (solar cell) or organic field-effect transistor. Conversely, a larger energy gap implies a greater kinetic stability but a lesser reactivity and conductivity [2].

The results clearly demonstrated that the anionic alpha molecular orbital of 9,10-DPA yielded a significantly smaller energy gap in comparison to the neutral and cationic counterparts, particularly with a band gap of about 1.3679eV, calculated using the basis set 6-311++G(d,p). Furthermore, it's evident that the neutral form of 9,10-DPA possesses the largest energy gap, measuring about 3.4540eV at 6-311++G(d,p) basis set. These observations suggest that neutral molecule is more stable and exhibit a greater aversion to donate electrons when compared to the ionic counterpart. Moreover, it's worth noting that the choice of basis set appears to have a relatively minor impact on the energy gap values compared to the influence of charging the molecules. These findings underscore the critical role of electron density and charge distribution in determining the conductivity, kinetic stability and reactivity of the molecule under investigation.

Table 3. The Frontier Orbital Energies for both Neutral and Ionic form of 9,10-Diphenylanthracene

NEUTRAL					
Molecule	Basis Set	MO	E_{HOMO} (eV)	E_{LUMO} (eV)	Energy Gap(eV)
9,10-DPA	6-31+G	Alpha	-5.3889	-1.9431	3.4458
	6-311++G	Alpha	-5.4556	-2.0016	3.4540
CATIONIC					
Molecule	Basis Set	MO	E_{SOMO} (eV)	E_{LUMO} (eV)	Energy Gap(eV)
9,10-DPA	6-31+G	Alpha	-9.2117	-6.1154	3.0963
		Beta	-10.0299	-7.8256	2.2043
	6-311++G	Alpha	-9.2895	-6.1786	3.1109
		Beta	-10.0971	-7.8980	2.1991
ANIONIC					
Molecule	Basis Set	MO	E_{SOMO} (eV)	E_{LUMO} (eV)	Energy Gap(eV)
9,10-DPA	6-31+G	Alpha	0.5165	2.2606	1.7441
		Beta	-1.2103	1.9248	3.1351
	6-311++G	Alpha	0.4620	1.8299	1.3679
		Beta	-1.2742	1.8282	3.1024

Ionization Potential (IP) and Electron Affinity (EA)

The ability of a molecule to accept or released an electron is determined by its ionization potential (IP) and the electron affinity (EA). The lower the electron affinity the less easy it is to add an electron and the higher the ionization potential (IP) the less easy it is to remove an electron [20]. The IPs and EAs of the neutral and ionic forms of the 9,10-DPA are presented in Table 4.

Table 4. The Ionization Potential (IP) and Electron Affinity of 9,10- Diphenylanthracene

Molecule	**Basis Set**	**MO**	**Neutral**		**Ionic**			
					Cationic		**Anionic**	
			IP (eV)	**EA (eV)**	**IP (eV)**	**EA (eV**	**IP (eV)**	**EA (eV)**
9,10-DPA	6-31+G	Alpha	5.39	1.94	9.21	6.12	-0.52	-2.26
		Beta	-	-	10.03	7.83	1.21	-1.92
	6-311++G	Alpha	5.46	2.00	9.29	6.18	-0.46	-1.83
		Beta	-	-	10.10	7.90	1.27	-1.83

The analysis reveals some interesting findings regarding the ionization potential (IP) and electron affinity (EA) of the studied molecule, specifically in its cationic state. It was observed that the cationic beta molecular orbital (MO) displayed the highest ionization potential, measuring 10.10eV when calculated using 6-311++G(d,p) basis set. This signifies that a substantial amount of energy is required to remove an electron from this particular molecular state. On the other hand, the molecule with the greatest electron affinity was also identified as the cationic beta MO, with an EA value of 7.90eV when calculated with the same basis set. This suggested that this molecule has a strong tendency to accept an additional electron. Comparing these cationic molecules to their neutral and anionic counterparts, it becomes apparent that the cationic forms exhibit higher ionization potentials and electron affinities. This implies that cationic molecules are more inclined to act as electron acceptors than electron donors.

Furthermore, this study highlighted that the ionization potential and electron affinity of the study molecules are more influenced by charging the molecules than the choice of basis set. These findings highlight the importance of taking into account the molecular charge state when evaluating ionization potential and electron affinity, as these factors significantly influence the electronic properties of the molecules.

Global Quantities of 9,10-Diphenylanthracene

The global chemical reactivity descriptors such as chemical hardness (η), chemical softness (S), electronegativity (χ), chemical potential (μ), and electrophilicity index (ω) were calculated from HOMO/SOMO and LUMO energies which were obtained at the level of theory B3LYP using the two basis sets 6-31+G(d) and 6-311++G(d,p) as depicted in Table 5.

Table 5. Global Chemical Reactivity Descriptors (GCRD) of 9,10- Diphenylanthracene

Neutral			
Property	Basis Set	MO	GCRD Value
η (eV)	6-31+G	Alpha	1.72
	6-311++G	Alpha	1.73
S (eV)	6-31+G	Alpha	0.58
	6-311++G	Alpha	0.58
χ (eV)	6-31+G	Alpha	3.67
	6-311++G	Alpha	3.73

μ (eV)	6-31+G	Alpha	-3.67
	6-311++G	Alpha	-3.73
ω (eV)	6-31+G	Alpha	3.90
	6-311++G	Alpha	4.02
Cationic			
Property	Basis Set	MO	GCRD Value
η (eV)	6-31+G	Alpha	1.55
		Beta	1.10
	6-311++G	Alpha	1.56
		Beta	1.10
S (eV^{-1})	6-31+G	Alpha	0.65
		Beta	0.91
	6-311++G	Alpha	0.64
		Beta	0.91
χ (eV)	6-31+G	Alpha	7.66
		Beta	8.93
	6-311++G	Alpha	7.73
		Beta	9.00
μ (eV)	6-31+G	Alpha	-7.66
		Beta	-8.93
	6-311++G	Alpha	-7.73
		Beta	-9.00
ω (eV)	6-31+G	Alpha	18.93
		Beta	36.25
	6-311++G	Alpha	19.23
		Beta	36.81
Anionic			
Property	Basis Set	MO	GCRD Value
η (eV)	6-31+G	Alpha	0.87
		Beta	2.94
	6-311++G	Alpha	0.68
		Beta	1.55
S (eV)	6-31+G	Alpha	1.15
		Beta	0.34
	6-311++G	Alpha	1.46
		Beta	0.64
χ (eV)	6-31+G	Alpha	-1.39
		Beta	-0.26
	6-311++G	Alpha	-1.15
		Beta	-0.28
μ (eV)	6-31+G	Alpha	1.39
		Beta	0.26
	6-311++G	Alpha	1.15
		Beta	0.28
ω (eV)	6-31+G	Alpha	1.11
		Beta	0.01
	6-311++G	Alpha	0.96
		Beta	0.02

Chemical Hardness (η) and softness (S) concepts are valuable for characterizing the properties of molecules, and these calculations provide insights into the relative hardness

and softness of 9,10-DPA, within the context of the chosen basis sets and molecular orbitals. A hard molecule exhibits a substantial energy gap, while a soft molecule features a smaller energy gap [21]. Consequently, soft molecules tend to be more polarizable than hard ones. Theoretical calculations have revealed interesting insights. In particular, the molecule that possess the highest hardness value is the anionic beta molecular orbital (η = 2.94 eV) when analysing using the 6-31+G(d) basis set. This designation signifies that it is the hardest molecule in the context of this study. Conversely, its anionic alpha molecular orbital stands out for having the highest chemical softness (S = 1.15eV) when calculated using the same basis set, 6-31+G(d). This observation highlights its distinction as the softest molecule within this study.

Electronegativity (χ) is a measure of a molecule's capacity to attract electrons. The values presented in table (4.5) clearly demonstrate that the cationic beta MO of 9,10-DPA exhibits the highest electronegativity value, approximately 9.00eV. This value surpasses that of all the other molecules as calculated using 6-311++G(d,p) basis set. This observation highlights the exceptional electron-attracting ability of the cationic beta MO of 9,10-DPA compared to the other molecules in the study [22]. Electronegativity is a fundamental concept in molecular reactivity, and the results provide valuable insights into the relative electron-attracting capabilities of these molecules.

The chemical potential (μ) serves as a measure of an electron's tendency to escape and can be correlated with molecular electronegativity. In this context, as μ becomes more negative, it indicates a higher resistance to electron loss but a greater ease in gaining electrons. The data presented in Table (4.5) demonstrates that the cationic beta molecular orbital of 9,10-DPA has a pronounced capacity to gain electrons, particularly evident when analysed using 6-311++G(d,p) basis set. This is supported by a chemical potential value of -9.00eV. Conversely, as revealed in Table (4.5) again, anionic alpha molecular orbital of 9,10-DPA, stands out as the least stable but most reactive and conductive among all the molecules under investigation. This conclusion is drawn from its notably high chemical potential value of 1.39eV, especially when employing the 6-31+G basis set.

In summary, the concept of chemical potential, as a measure of electron tendencies, provides valuable insights into the relative stabilities and reactivities of these molecules [22]. The data suggests that the cationic beta molecular orbital 9,10-DPA has a strong

inclination to gain electrons, while the anionic alpha molecular orbital 9,10-DPA, exhibits higher reactivity due to its elevated chemical potential value.

Electrophilicity (ω) is a concept that provides insight into the energy of stabilization when a system becomes saturated with electrons from the external environment. This reactivity information helps determine a molecule's ability to donate charge. A molecule with a lower ω value is considered a strong nucleophile, indicating heightened reactivity in donating electrons, while higher ω values suggest the presence of a potent electrophile, capable of accepting electrons [22]. Our findings reveal interesting trends. Specifically, the anionic beta molecular orbital exhibits low ω values of approximately 0.01eV when analysed using the 6-31+G basis set. This observation characterizes it as a proficient nucleophile, highlighting its capacity to donate charge effectively. In contrast, the cationic beta molecular orbital exhibits a significantly higher ω value, approximately 36.81eV, as determined with the 6-311++G basis set. This elevated ω value characterizes it as a strong electrophile, indicating its ability to readily accept electrons.

IR Spectra

Vibrational frequency analysis is a vital technique used to elucidate the vibrational characteristics of specific molecular structures within a compound. Molecular vibrations occur when atoms within a molecule engage in periodic motion while the molecule, as a whole, maintains translational and rotational motion. The frequency at which this periodic motion occurs is referred to as the vibrational frequency [15].

In the present study, vibrational frequencies were computed for 9,10-DPA, using Density Functional Theory (DFT) with the B3LYP exchange functional under 6-31+G(d) and 6-311++G(d,p) basis sets. The resulting infrared spectra were generated using Gauss View software, as illustrated in Figs. 2-4.

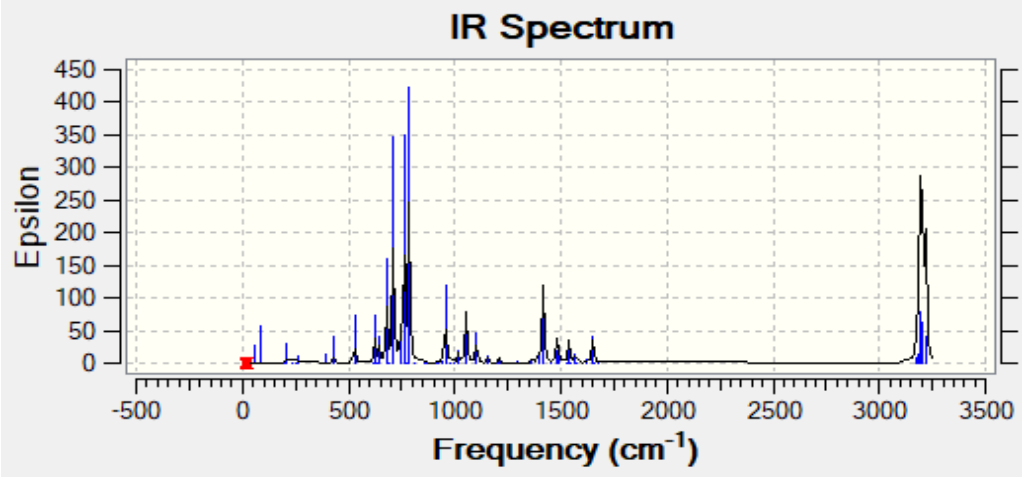

(a)

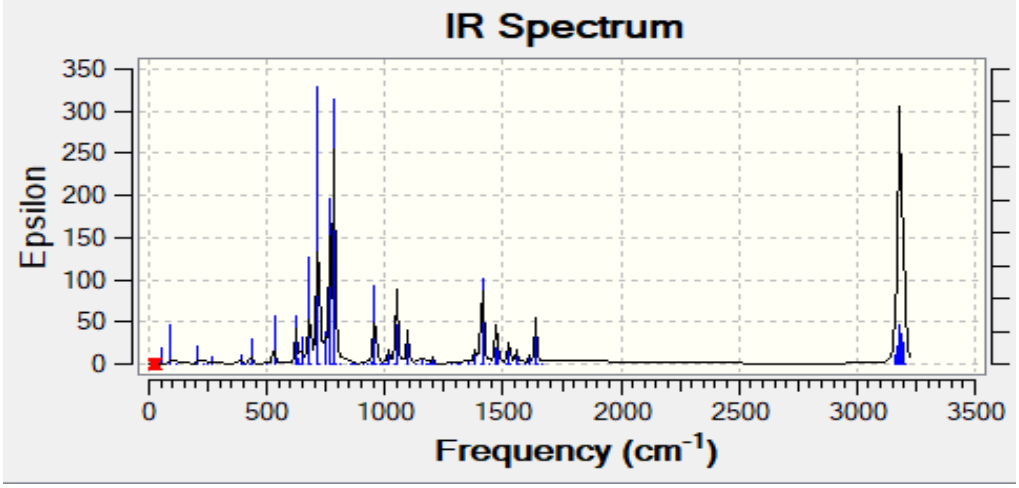

(b)

Figure 2. (a) Neutral 9,10-DPA(1), (b) Neutral 9,10-DPA(2)

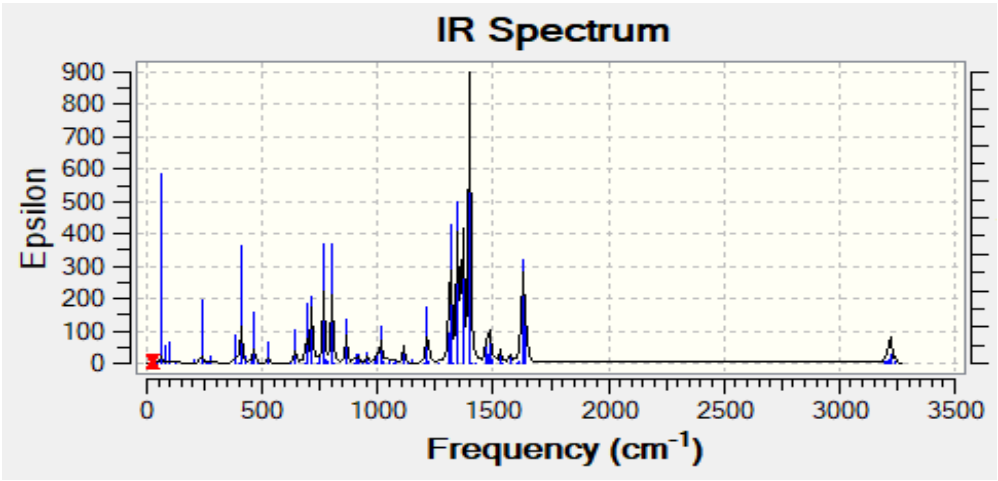

(a)

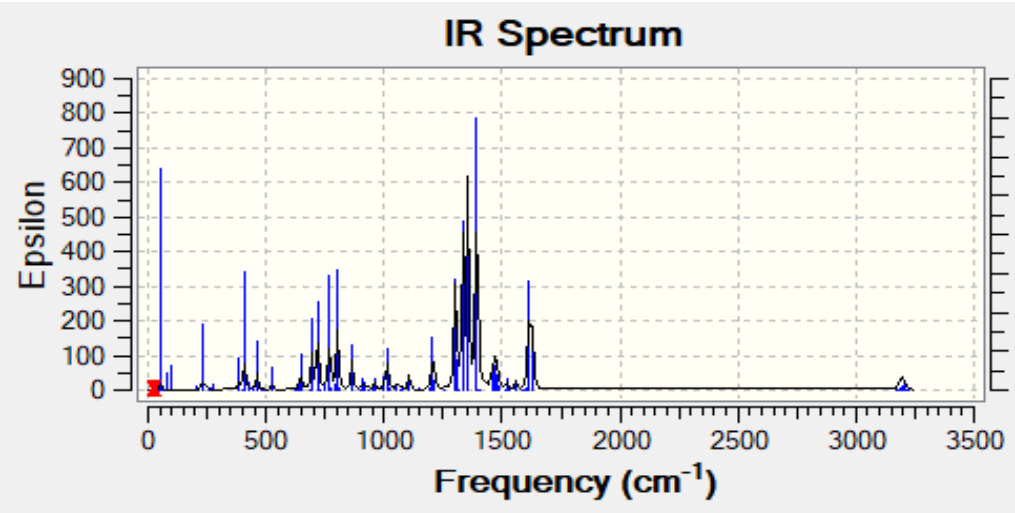

(b)

Figure 3. (a) Cationic 9,10-DPA(1), (b) Cationic 9,10-DPA(2)

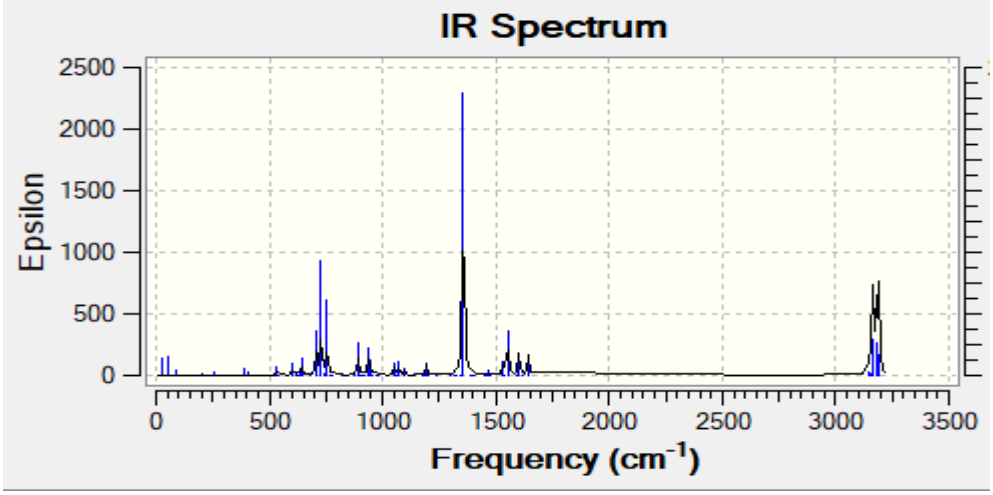

(a)

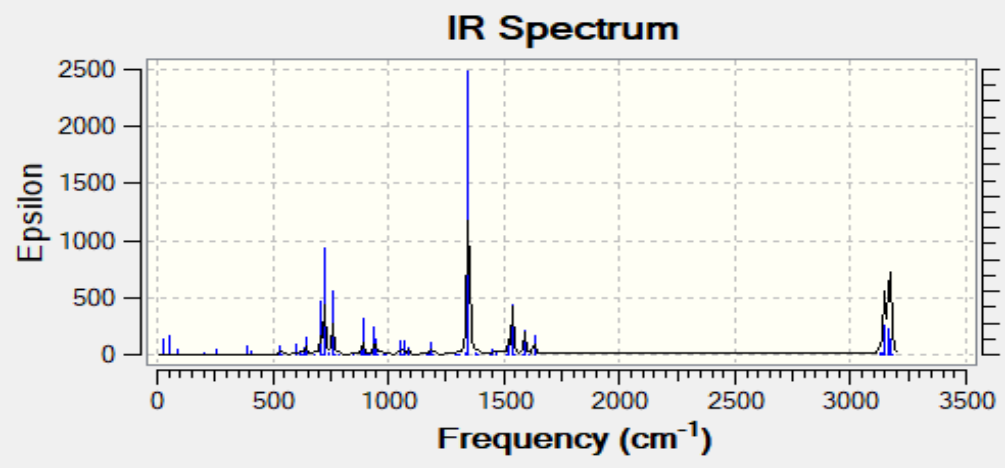

(b)

Figure 4. (a) Anionic 9,10-DPA(1), (b) Anionic 9,10-DPA(2)

Figs. 2 (a)-(b) shows the IR spectrum of neutral 9,10-Diphenylanthracene under the two basis sets employed in this research, from the figures we observed the highest intense IR absorption (about ε = 425 $Lmol^{-1}cm^{-1}$) at a frequency around 785.545cm^{-1} in the first basis set and that of the second basis set is at frequency around 716.514cm^{-1} and has an absorption intensity (about 330 $Lmol^{-1}cm^{-1}$) which is less than that of the first basis set.

Figs. 3 (a)-(b) shows the IR spectrum of cationic 9,10-Diphenylanthracene under the two basis sets employed in this research, from the figures we observed the highest intense IR absorption (about 900 $Lmol^{-1}cm^{-1}$) at a frequency around 1398.26cm^{-1} in the first basis set and that of the second basis set is at frequency around 1393.14cm^{-1} and has an absorption intensity (about 790 $Lmol^{-1}cm^{-1}$) which is less than that of the first basis set.

Figs. 4 (a)-(b) shows the IR spectrum of cationic 9,10-Diphenylanthracene under the two basis sets employed in this research, from the figures we observed the highest intense IR absorption (about 2300 Lmol-1cm-1) at a frequency around 1356.54cm-1 in the first basis set and that of the second basis set is at frequency around 1346.96cm-1 and has an absorption intensity (about 2500 Lmol-1cm-1) which is greater than that of the first basis set.

Notably, the most intense vibrational frequency for 9,10-DPA was observed in its anionic form using 6-311++G(d,p) basis set at 1346.96cm^{-1} having the highest absorption

value (figure 4b). The above data indicates that the anionic 9,10-DPA has higher Infrared absorption compared to the remaining molecules. The symmetric stretching modes were observed in the spectral region below 3100 cm^{-1}, while the spectral region between 3100 and 3500 cm^{-1} featured the asymmetric stretching modes of vibration.

For these aromatic molecules, the in-plane vibrations were discerned in the frequency range of 1250-1750cm^{-1}, while the out-of-plane vibrations manifested below 1200cm^{-1} for the ionic forms of 9,10-DPA. In the case of its neutral forms, the in-plane vibrations were observed in the frequency range between 500-900cm^{-1}, and the out-of-plane vibrations were evident between 900 - 1750cm^{-1}. In conclusion, the analysis suggests that anionic 9,10-DPA molecules possess the highest level of infrared (IR) absorption by exhibiting the highest peaks in the vibrational modes among other molecular state.

4 Conclusions

This study delved into the structural, electronic properties, and infrared absorption capabilities of 9,10-DPA, offering valuable insights into how molecular behaviour is influenced by charging. The analysis of bond lengths and angles emphasized that the following bond length R(C_7-H_{18}), R(C_8-H_{19}), R(C_{12}-H_{26}) and R(C_{13}-H_{27}) exhibits greater bond energy and strength in both neutral and ionic stats because of having shorter bond length than the remaining regardless of the chosen basis set. The exploration of molecular orbitals and their energy gaps provided further insights into the electronic properties of the molecules under study. The smaller HOMO-LUMO energy gaps obtained in the ionic molecules (specifically the anionic alpha MO) indicates lower stability but higher reactivity and conductivity. This further indicates its greater tendency to donate electrons which makes it a better semiconductor among other molecular state. In the other hand, larger HOMO-LUMO energy gap values for neutral molecules implies a greater stability and a lower tendency to donate electrons compared to its ionic counterpart. In the case of global chemical reactivity descriptors (GCRDs), the hardest molecular orbital (MO) was found to be the anionic beta MO which occurred as the result of having the highest hardness value among all the MO, the MO with the highest reactivity was found to be anionic alpha MO because it exhibits higher chemical potential as well as higher softness

value. In the other, cationic beta MO was found to have the highest electron-attracting capability because of having the highest electronegativity value, lower and negative chemical potential (making it to have higher resistance to release electrons but greater ease in gaining electrons) and also considered to be strong electrophile because it possessed the highest electrophilicity index (it has the greater ability to accept electrons). The analysis of IR spectra suggests that anionic 9,10-DPA molecules possess the highest level of infrared (IR) absorption by exhibiting the highest peaks in the vibrational modes among other molecular state. In general, the results show a great novelty by contributing into a deeper understanding of the complex and delicate interaction or relationship between structure, stability, conductivity and reactivity in aromatic molecules. The findings emphasize the critical role of charge states in shaping these characteristics. These insights are crucial for advancing our understanding of molecular behaviour and for potential applications in various scientific and technological domains.

References

1. Ren, Z. (2010). Molecular Vibration and Charge Transport in Crystalline Oligoacenes and Derivatives: Raman and DFT Combined Study. Chapel Hill: University of North carolina.
2. Abubakar, A. A., Suleiman, A. B., & Gidado, A. S. (2021). Density Functional Theory Investigation of the Doping Effects of Bromine and Fluorine on the Electronic and Optical Properties of Neutral and Ionic Perylene. Physical Science International Journal, 1-13.
3. Hiszpanski, A. M., & Loo, Y. L. (2014). Directing the film structure of organic semiconductors via post-deposition processing for transistor and solar cell applications. Energy Environ. Sci, vol. 7, 592-608.
4. Sano, M., Pope, M., & Kallmann, H. (1965). Electroluminescence and Band Gap in Anthracene. Journal of Chemical Physics: Bibcode: 1965JChPh. 43.2920S. doi:10.1063/1.1697243, 2920-2921.

5. Arias, A. C., MacKenzie, J. D., McCulloch, I., Rivnay, J., & Salleo, A. (2010). Materials and Applications for Large Area Electronics: Solution-Based Approaches. In Chemical Reviews (pp. 3-24). American Chemical Society.
6. Martin-Palma, R. J., & Martinez-Duart, J. (2017). Nanotechnology for Microelectronics and Photonics (Second Edition). Elsevier Science.
7. Rajeswara, R. M., Hayden, T. B., & Dmitrii, F. P. (2015). Synthesis and Divergent Electronic Properties of Two Ring-Fused Derivatives of 9,10-Diphenylanthracene. Organic letters: American Chemical Society. DOI: 10.1021/acs.orglett.5b02009, A-D.
8. Bruetting , W. (2005). Physics of Organic Semiconductors, 1-14. https://doi.org/10.1002/3527606637.ch. Weinheim: WILEY-VCH Verlag GmbH and Co. KGaA.
9. Watanabe, S., Shimodo, Y., & Morihashi, K. (2011). Theoretical investigation of hole mobility in 9,10-diphenylanthracene by density functional calculations. Theor. Chem. Acc. Vol. 130:807–813. DOI 10.1007/s00214-011-1042-5, 807-813.
10. Yating, S., Yarui, S., Huiling , W., Hongsheng. , Z., & Yufang, L. (2017). A theoretical Study on Electronic Properties of Two Ring-Fused Derivatives of 9, 10-Diphenylanthracene. Royal Society of Chemistry: New Journal of Chemistry: DOI: 10.1039/C7NJ02590D, 1-22.
11. Ndikilar, C. E., Gidado, A. S., Suleiman, A. B., & Maigari, A. (2022). Effects of Mono-Halogen-Substitution on the Electronic and Non-Linear Optical Properties of Poly (3-hexylthiophene-2, 5-diyl) for Solar Cell Applications: A DFT Approach. Journal of Energy Research and Reviews, 1-14.
12. Ajeel, F. N., Khudhair, A. M., & Mohammed, A. A. (2013). Density Functional Theory Investigation of the Physical Properties of Dicyano Pyridazine Molecules. International Journal of Science and Research (IJSR), 4(1). ISSN (Online): 2319-7064, 2334-2339.
13. Abdulaziz, H., Gidado, A. S., Musa, A., & Lawal, A. (2019). Electronic Structure and Non-Linear Optical Properties of Neutral and Ionic Pyrene and Its Derivatives

Based on Density Functional Theory. Journal of Materials Science Research and Reviews; Article no.JMSRR.45683, 1-13.

14. Gobre, V. V. (2016). Efficient modelling of linear electronic polarization in materials using atomic response functions. Berlin (Germany): Technische Universitaet.
15. Musa, A., Gidado, A. S., Mohammed , L., Yunusa , K., & Suleiman, A. B. (2019). Molecular and Electronic Properties of Rubrene and Its Cyanide Derivative Using Density Functional Theory (DFT). Musa, A., Gidado, A.S., IOSR Journal of Applied Physics (IOSR-JAP), 11(2), ., 10-18.
16. Becke, A. D. (1992). Density-functional thermochemistry. III. The role of exact exchange. The journal of chemical Physics, 5648-5652.
17. Ketkar, S. N., Kelley, M., Fink, M., & Ivey, R. C. (1981). An Electron Diffraction Study of the Structures of Anthraquinone and Anthracene. Journal of Molecular Structure, Elsevier Scientific Publishing Company, Amsterdam - printed in the Netherlands, 127-138.
18. Sulaiman, N. M., Taura, L. S., Lawal, A., Gidado, A. S., & Musa, A. (2019). Solvent Effects on the Structural, Electronic, NonLinear Optical and Thermodynamic Properties of Perylene Based on Density Functional Theory. Journal of Materials Science Research and Reviews, 1-13.
19. Ling-Ping, X., Guo-Hua, Z., Zhi, Z., & Xiao, J. (2015). Theoretical study on structural and electronic properties of solid anthracene under high pressure by density functional theory. Molecular Physics. Moecular Physics (International Journal at the Interface between chemistry and physics), 1-7.
20. Kumer, A., Ahmed, B., Sharif, M., & Al-mamun, A. (2017). A Theoretical Study of Aniline and Nitrobenzene by Computational Overview. Asian Journal of Physical and Chemical Sciences .https://doi.org/10.9734/AJOPAC S/2017/38092, 1-12.
21. Taura, L. S., Muhammad, R. N., Lawal, A., & Gidado, A. S. (2022). Electronic Structure and IR Spectra Analysis of Tetrathiafulvelene (TTF) Using RHF and DFT Quantum Mechanical Methods. Journal of Energy Research and Reviews. 10(4): 20-35; Article no.JENRR.84391, 20-35.

22. Muhammad, R. N., Mahraz, N. M., Gidado, A. S., & Musa, A. (2021). Theoretical Study of Solvent Effects on the Electronic and Thermodynamic Properties of Tetrathiafulvalene (TTF) Molecule Based on DFT. Asian Journal of Research and Reviews in Physics. Articlle no.AJR2P.77309, 42-54.